TLR9 Activation Induces Normal Neutrophil Responses in a Child with IRAK-4 Deficiency: Involvement of the Direct PI3K Pathway

Cyrille Hoarau,*† Bénédicte Gérard,‡§ Emmanuel Lescanne,† Dominique Henry,§ Stéphanie François,‡§¶ Jean-Jacques Lacapère,‡¶ Jamel El Benna,‡¶ Pham My-Chan Dang,‡¶ Bernard Grandchamp,‡§ Yvon Lebranchu,*† Marie-Anne Gougerot-Pocidalo,‡§¶ and Carole Elbim[1]‡§¶

Polymorphonuclear neutrophils (PMN) play a key role in innate immunity. Their activation and survival are tightly regulated by microbial products via pattern recognition receptors such as TLRs, which mediate recruitment of the IL-1R-associated kinase (IRAK) complex. We describe a new inherited IRAK-4 deficiency in a child with recurrent pyogenic bacterial infections. Analysis of the *IRAK4* gene showed compound heterozygosity with two mutations: a missense mutation in the death domain of the protein (pArg^{12}Cys) associated in *cis*-with a predicted benign variant (pArg^{391}His); and a splice site mutation in intron 7 that led to the skipping of exon 7. A nontruncated IRAK-4 protein was detected by Western blotting. The patient's functional deficiency of IRAK-4 protein was confirmed by the absence of IRAK-1 phosphorylation after stimulation with all TLR agonists tested. The patient's PMNs showed strongly impaired responses (L-selectin and CD11b expression, oxidative burst, cytokine production, cell survival) to TLR agonists which engage TLR1/2, TLR2/6, TLR4, and TLR7/8; in contrast, the patient's PMN responses to CpG-DNA (TLR9) were normal, except for cytokine production. The surprisingly normal effect of CpG-DNA on PMN functions and apoptosis disappeared after pretreatment with PI3K inhibitors. Together, these results suggest the existence of an IRAK-4-independent TLR9-induced transduction pathway leading to PI3K activation. This alternative pathway may play a key role in PMN control of infections by microorganisms other than pyogenic bacteria in inherited IRAK-4 deficiency. ***The Journal of Immunology,*** **2007, 179: 4754–4765.**

Polymorphonuclear neutrophils (PMN)[2] play a key role in host defense against bacterial and fungal pathogens (1). They contribute to early innate response by rapidly migrating into inflamed tissues, where their activation triggers microbicidal mechanisms such as release of proteolytic enzymes and antimicrobial peptides, and rapid production of reactive oxygen species (ROS), in the so-called oxidative burst. PMN die spontaneously by apoptosis and are then recognized and phagocytosed by macrophages (2).

*Unité de Formation et de Recherche de Médecine, Cellules Dendritiques et Greffes, Université François Rabelais, Tours, France; †Unité Transversale d'Allergologie, Néphrologie et Immunologie Clinique et Service d'Oto-Rhino-Laryngologie, Centre Hospitalier Universitaire de Tours, Tours, France; ‡Faculté de Médecine, site Bichat, Université Paris 7, Paris, France; §Assistance Publique-Hôpitaux de Paris, Service d'Immunologie et d'Hématologie et Service de Biochimie Hormonale et Génétique, Centre d'Investigation Biomédical Phenogen, Centre Hospitalier Universitaire Xavier Bichat, Paris, France; and ¶Institut National de la Santé et de la Recherche Médicale Unité 773, Paris, France

Received for publication April 12, 2007. Accepted for publication July 22, 2007.

The costs of publication of this article were defrayed in part by the payment of page charges. This article must therefore be hereby marked *advertisement* in accordance with 18 U.S.C. Section 1734 solely to indicate this fact.

[1] Address correspondence and reprint requests to Dr. Carole Elbim, Institut National de la Santé et de la Recherche Médicale Unité 773, Faculté Xavier Bichat, 16 rue Henri Huchard, Paris, France. E-mail address: carole.elbim@bch.aphp.fr

[2] Abbreviations used in this paper: PMN, polymorphonuclear neutrophil; ROS, reactive oxygen species; IRAK, interleukin-1 receptor-associated kinase; TIR, Toll-IL-1 receptor; TRAF6, TNFR-associated factor 6; MALP-2, macrophage-activating lipopeptide-2; HE, hydroethidin; 7-AAD, 7-aminoactinomycin D; Pam3CSK4, palmitoylated mimic of bacterial lipopeptides; CBA, cytometric bead array; LNA, locked nucleic acid; MFI, mean fluorescence intensity.

PMNs directly recognize microbial products via pattern recognition receptors such as TLRs. Human PMNs have been reported to express all TLRs except TLR3 (3); TLR5 and TLR7 are weakly expressed (4). TLRs are members of the IL-1R superfamily, characterized by an intracytoplasmic Toll-IL-1 receptor (TIR) domain which mediates recruitment of the IL-1 receptor-associated kinase (IRAK) complex via TIR-containing adapter molecules such as MyD88. During formation of this complex, IRAK-4 is activated, leading to hyperphosphorylation of IRAK-1, which in turn induces the interaction of TNFR-associated factor 6 (TRAF6) with the complex. TRAF6 then triggers downstream signaling, and this results in NF-κB activation (5, 6). In addition, TLR engagement activates stress kinases such as MAP kinases, JNK, and PI3K in most cells, including PMNs (7, 8). The PI3K pathway has variously been shown to regulate TLR-mediated inflammatory responses, through negative feedback functions (9, 10), or to enhance NF-κB nuclear translocation (11, 12). In particular, it was recently suggested that the PI3K signaling cascade occupies a central role in TLR2-induced activation of PMN (13).

PMN stimulation through TLRs causes an immediate defensive response, including modulation of adhesion molecule expression (L-selectin shedding and β_2-integrin up-regulation), production of an array of antimicrobial molecules (ROS and cytokines) (3, 13), and inhibition of apoptosis (4). The major role of the TIR-IRAK signaling pathway in immunity to infections by pyogenic bacteria is illustrated by the recent descriptions of children with inherited IRAK-4 deficiency associated with recurrent infections (14–22). The cells of these patients fail to respond to IL-1 and IL-18 and to the stimulation of at least five TLRs (TLR2, TLR3, TLR4, TLR5, TLR9).

Here we describe a case of inherited IRAK-4 deficiency related to new double-heterozygous mutations generating a nonfunctional IRAK-4 protein. We show that some PMN functions (adhesion molecule expression, ROS production, survival) that are critical for antimicrobial defenses occur normally in response to CpG-DNA (TLR9), despite an impaired response to the other TLR agonists, suggesting the existence of a distinct TLR9-induced transduction pathway.

Materials and Methods

Case reports

We investigated a 14-year-old boy with recurrent infections, osteomyelitis, and cellulitis. He was born in July 1991 and was the second child of healthy unrelated parents. There was no family history of recurrent or severe infections, autoimmune disease, or lymphoma. His brother and sister were healthy. At age 15 days, he developed a severe necrotic infection of his palate, due to *Pseudomonas aeruginosa*. Despite several surgical procedures, he had velopharyngeal insufficiency and recurrent otitis media. Vaccines were normally tolerated. From the age of 5 years, he had severe chronic otitis media, arthritis, and impetigenous infections of the face and limbs, usually after skin trauma. Local and systemic antibiotics were usually necessary to eradicate the infections. At age 9 years, he underwent tympanoplasty for tympanic membrane perforation, which was complicated by retroauricular cellulitis due to *Staphylococcus aureus*, and severe impetigo of the face and hands, leading to graft loss. The procedure failed to close the tympanic perforation. At age 10 years, he was hospitalized for cervical adenitis associated with fatigue and weight loss. The CRP was elevated at 24 mg/ml. The PMN count was reduced at 920/mm^3, but the chest radiograph and tuberculin test were normal. Serological tests for *Bartonella*, *Borrelia,* and Lyme's disease were negative. Surgical biopsy showed nonspecific subacute lymphadenitis. The adenitis regressed on amoxicillin + clavulanic acid. At age 14 years, he developed asthma and common verrucas. Chest radiography and computed tomography were normal. Inhaled steroid therapy and smoking cessation improved his bronchospasm. Prophylactic antibiotic therapy with sulfamethoxazole + trimethoprim was started, and he underwent a second tympanic repair, without infectious complications.

His growth and development were normal. He had no severe viral or fungal infections or infections due to intracellular bacteria.

Immunological studies gave normal results (lymphocyte counts: CD3$^+$ 2037/mm^3, CD4$^+$ 1328/mm^3, CD8$^+$ 798/mm^3, CD19$^+$ 798/mm^3, CD16$^+$ 321/mm^3; IgA 1.27 g/L; IgG 12.08 g/L (IgG1 10 g/L, IgG2 2.52 g/L, IgG3 0.72 g/L, IgG4 0.05 g/L); IgM 1.38 g/L) excepted for a still low number of PMN. The complement system was normal.

PMN migration was normal when tested with the under-agarose method, with and without fMLP (10^{-7} M) and activated serum (23), ruling out leukocyte adhesion deficiency. PMN phagocytosis of *Staphylococcus epidermidis* was normal, as was PMN chemiluminescence after stimulation with PMA (100 ng/ml), ruling out a chronic granulomatous disease.

Reagents

The reagents and sources were as follows: ultrapurified LPS from *Escherichia coli* serotype R515 (LPS) and synthetic macrophage-activating lipopeptide-2 (MALP-2; Alexis); R-848 and a synthetic palmitoylated mimic of bacterial lipopeptides (Pam3CSK4; Invivogen); unmethylated CpG-DNA (HyCult Biotechnology); hydroethidine (HE; Fluka); fMLP, PMA, and ionomycin (Sigma-Aldrich); SN50, SB203580, PD98059, genistein, wortmannin, rottlerin, and GF109203X (Calbiochem); allophycocyanin-conjugated annexin V, 7-aminoactinomycin D (7-AAD), fluorescein (FITC)-anti-CD15, purified anti-L-selectin and FITC-conjugated goat anti-rabbit Abs, PE-conjugated anti-phosphorylated p38MAPK and ERK1/2 Abs, and cytometric bead array (CBA) kit (BD Pharmingen); PE-conjugated anti-CD45 Ab (Immunotech); PE-conjugated anti-CD11b Ab (Dakopatts); FITC-conjugated goat anti-mouse Ab (Nordic Immunology); anti-IRAK-4, anti-phospho-IRAK-1 and anti-phospho-Bad (S136) Abs (Cell Signaling Technology); anti-Mcl-1 Ab (Santa Cruz Biotechnology); TNF-α and GM-CSF (R&D Systems); IL-18 (MBL).

Incubation of whole blood with TLR agonists

One-milliliter aliquots of fresh blood, collected on lithium heparinate (10 U/ml), were incubated at 37°C for various times with PBS, IL-18 (500 ng/ml), or the following TLR agonists (reported to stimulate PMN functions) (4): LPS (10 ng/ml; TLR4); MALP-2 (10 ng/ml; TLR2/6); Pam3CSK4 (500 ng/ml; TLR1/2); R-848 (10 μg/ml; TLR7/8); and CpG-DNA (100 μg/ml; TLR9). These optimal concentrations were determined in preliminary concentration-response experiments (C. Elbim, personal data).

In some experiments, samples were pretreated with the NF-κB inhibitor SN50 (100 μg/ml) or kinase inhibitors at optimal concentrations previously determined in whole blood (wortmannin, 2500 nM; LY2940002, 25 μM; GF109203X, 5 μM; genistein, 100 μM; PD98059, 50 μM; SB203580, 25 μM; rottlerin, 10 μM; see Ref. 4).

Determination of adhesion molecule expression at the PMN and monocyte surface

Whole-blood samples were either kept on ice or incubated at 37°C for 1 h with PBS, IL-18, or TLR agonists as described above; TNF-α (100 U/ml) was used as control. Samples (100 μl) were then stained at 4°C for 30 min with PE-anti-human CD11b or purified anti-L-selectin Abs. To study L-selectin expression, samples were then washed with ice-cold PBS and incubated at 4°C for 30 min with FITC-goat anti-mouse Ab. RBC were lysed with FACS lysing solution (BD Biosciences) and white blood cells were resuspended in 1% paraformaldehyde-PBS. Nonspecific Ab binding was determined on cells incubated with the same concentration of an irrelevant Ab of the same isotype.

NADPH oxidase activity in priming conditions

Superoxide anion (O_2^-) production was measured with a flow cytometric assay derived from the HE oxidation technique (24): Whole-blood samples (500 μl) were loaded for 15 min with HE (1500 ng/ml) at 37°C and then incubated with PBS, IL-18, or TLR agonists as described above; TNF-α (100 U/ml) was used as positive control; samples were then treated with PBS or 10^{-6} M fMLP for 5 min. RBC were lysed as described above and white blood cells were resuspended in 1% paraformaldehyde-PBS.

Measurement of PMN apoptosis

Apoptosis of PMN in whole blood was quantified by using annexin V and 7-AAD (an impermeant nuclear dye) as previously described (4, 25). Samples were incubated in 24-well tissue cultures plates at 37°C with 5% CO_2 for 8 h with PBS, IL-18, or TLR agonists as described above; GM-CSF (1000 pg/ml) was used as an antiapoptotic control. Samples (100 μl) were washed twice in PBS, incubated on ice with FITC-anti-CD15 and PE-anti-CD45 Abs for 15 min, and then with allophycocyanin-annexin V for 15 min. After dilution in PBS (500 μl), samples were incubated with 7-AAD at room temperature for 15 min and analyzed immediately by flow cytometry. PMN were identified as CD15^{high} cells. Use of the combination of allophycocyanin-annexin V and 7-AAD distinguishes between early apoptotic PMN (annexin V$^+$, 7-AAD$^-$) and late apoptotic PMN (annexin V$^+$, 7-AAD$^+$).

Study of intracellular phospho-IRAK-1, phospho-p38MAPK, phospho-ERK1/2, and Bcl-2 family protein content by flow cytometry

After incubation of whole blood with TLR agonists or PBS for various times at 37°C, leukocytes were permeabilized in 90% methanol as previously reported (4, 26). Cells were then stained with anti-IRAK-1 phospho-specific, anti-Mcl-1 or anti-Bad phospho-specific Abs for 1 h at room temperature and washed once in PBS, 2% human serum albumin. Samples were then incubated for 30 min with FITC-goat anti-mouse or anti-rabbit Ab. Phospho-p38MAPK and phospho-ERK1/2 contents were studied by staining with PE-conjugated anti-phospho-p38MAPK and phospho-ERK1/2 Abs. After one wash, leukocytes were resuspended in 1% paraformaldehyde-PBS.

Cytokine production by blood cells

Blood PMN were isolated in LPS-free conditions in medium containing 9% Dextran T-500 (Pharmacia) and 38% Radioselectan (Schering); the leukocyte suspension was then centrifuged on Ficoll-Paque medium (Pharmacia). The cell pellet was washed with PBS, and erythrocytes were removed by hypotonic lysis; PMN were further purified by negative selection with pan anti-human HLA class II-coated magnetic beads (Miltenyi Biotec) to deplete B lymphocytes, activated T lymphocytes, and monocytes as previously described (27). Fewer than 0.5% of cells were positive by nonspecific esterase staining, and flow cytometry showed the absence of CD45$^+$CD14^{high}, CD45$^+$CD3$^+$, and CD45$^+$CD19$^+$ cells; this showed that the PMNs were highly purified, without contaminating monocytes. In parallel, the mononuclear cell ring obtained after Ficoll-Paque centrifugation was treated with anti-CD14-coated magnetic beads (Miltenyi Biotec) to positively select monocytes.

Whole blood, pure PMNs (5×10^6/ml), or pure monocytes (5×10^5/ml) were cultured for 18 h at 37°C with 5% CO_2 in 24-well tissue culture plates

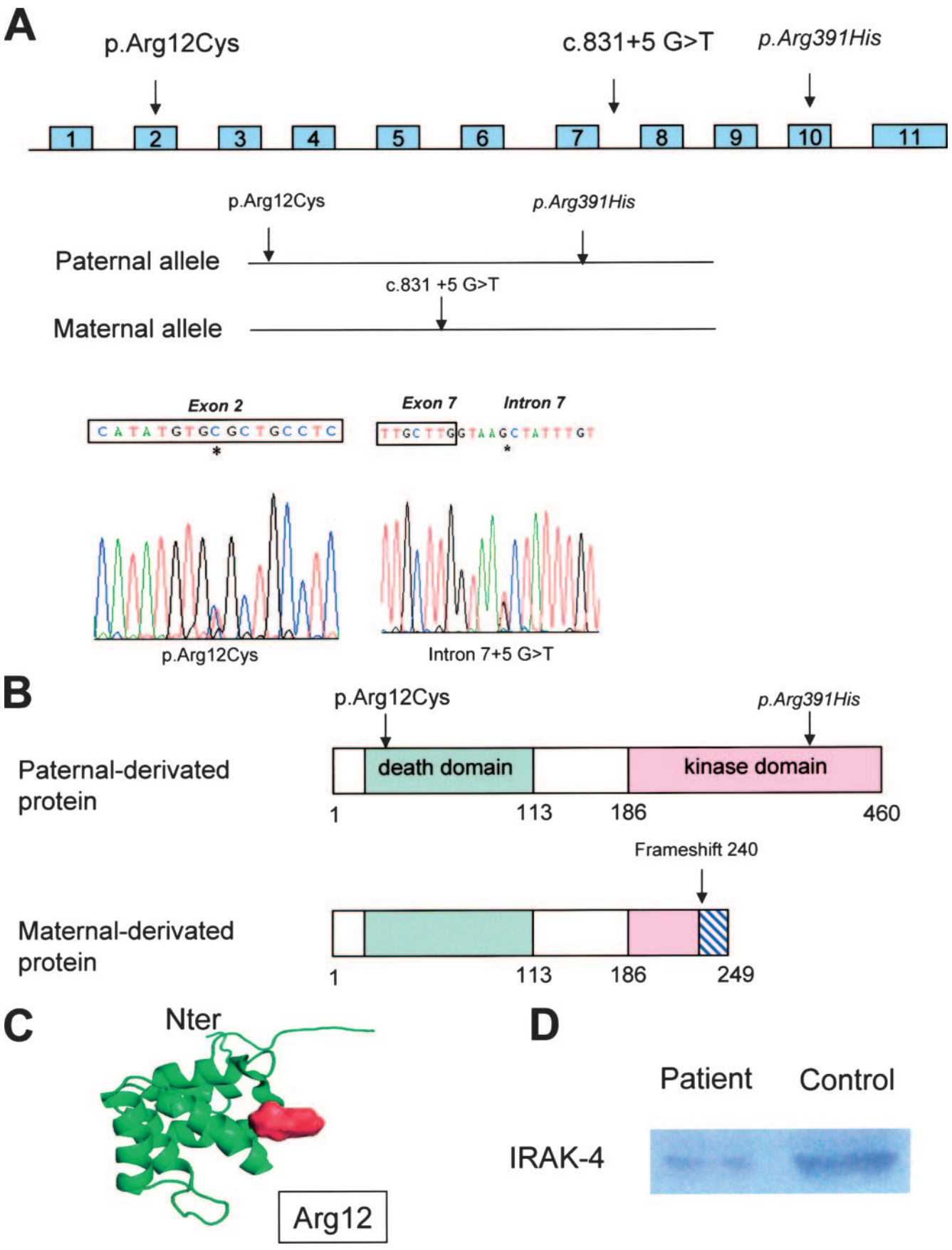

FIGURE 1. Genetic analysis of *IRAK4* gene and protein expression in the patient. *A,* Schematic representation of the *IRAK4* gene and alleles in the patient. Sequencing chromatograms obtained in our patient are shown. *B,* Schematic representation of IRAK-4 protein, with the death domain and kinase domain. The positions of the mutations found in the patient are indicated. *C,* Schematic representation of the IRAK-4 death domain (Protein Data Bank accession code 2A9I). This ribbon diagram was generated with PyMOL (DeLano Scientific, www.pymol.org). The Arg^{12} is shown as a full-surface amino

(Costar) in RPMI 1640 (Sigma-Aldrich). TLR agonists, IL-1β, and IL-18 were added to the culture medium. PMA (100 ng/ml) and PMA (100 ng/ml) + ionomycin (10^{-5} M) were used as positive controls. Supernatants were stored at −70°C for no longer than 15 days before assay. IL-8, IL-6, IL-1β, and TNF-α were detected simultaneously in supernatants by using the human inflammatory cytokine cytometric bead array (CBA) kit (BD Pharmingen). The CBA working range was 20–5000 pg/ml for each cytokine.

Flow cytometry

We used a BD Biosciences FACSCalibur (Immunocytometry Systems) with a 15-mW, 488-nm argon laser and a 635-nm diode laser. PMN functions were analyzed using CellQuest software. To measure apoptosis in whole blood, PMNs were identified on the CD15/SSC dot plot, and 2×10^5 events were counted per sample. In other experiments, forward and side scatter were used to identify the PMN population and to gate out other cells and debris; 10^4 events were counted per sample. Plasma cytokine levels were analyzed with CBA software (BD Pharmingen).

Blot analysis of IRAK-4

PMN were isolated and highly purified as described above. Suspensions of 40×10^6 PMNs/ml in PBS buffer were incubated with PBS or TLR agonists for 5 min and treated with 2.7 mM diisopropylfluorophosphate for 20 min at 4°C and then pelleted at $400 \times g$ for 8 min at 4°C (28). The pellet was resuspended in CHAPS solubilization buffer containing 50 mM Tris (pH 7.5), 15 mM CHAPS, 1 mM EDTA, and antiproteases. The cells were incubated on ice, and the suspension was then centrifuged at $1500 \times g$ for 5 min. Following SDS-PAGE on 10% acrylamide gels, the proteins were transferred to nitrocellulose filters. The filters were incubated for 1 h at room temperature in 50 mM Tris, 150 mM NaCl, 0.1% Tween 20 (TBST) containing 5% (w/v) fat-free dried milk. The nitrocellulose membranes were incubated overnight with anti-IRAK-4 Ab at 1/500 dilution. After five washes with TBST, the membranes were incubated with goat anti-mouse or goat anti-rabbit Abs conjugated to HRP. After five more washes with TBST, the blots were revealed with a chemiluminescence method (ECL; Amersham Life Sciences) following the manufacturer's instructions.

Genetic analysis

The propositus and his parents underwent genetic analysis with their written informed consent. DNA and RNA were extracted from whole blood with Qiagen extraction kits following the manufacturer's instructions. The *IRAK4* coding sequence and intron-exon junctions were sequenced in the patient and his parents (PCR conditions and primers are available on request), using an ABI sequencing kit (Applera) and a 3130xl DNA sequencer (Applera). cDNA was analyzed after reverse transcription of the patient's RNA by PCR using sets of primers located in various exons (Ex6F cDNA: CTACTGAAGAACTGAAACAG CAGTTTGA; Ex7F cDNA: GTTTACATGCCTAATGGTTCATTGC; Ex11R cDNA: CGACATTGGCTAGCACCAGAGTA). Forward primers were 6-FAM-labeled. Allele-specific amplification of cDNA was performed using modified oligonucleotides (the 3′-end nucleotide is one locked nucleic acid (LNA) molecule from Proligo; Ex10R LNA_G: CTAGCAATAACTGAGGTTCAC; Ex10R LNA_A: TATCTAGCAAT AACTGAGGTTCAT). Analysis of the fluorescent PCR products was done with a 310 DNA sequencer (Applera).

Statistical analysis

Data are reported as means ± SEM. Comparisons were based on ANOVA and Tukey's post hoc test, using Prism 3.0 software (Graph Pad software).

Results

IRAK4 *mutations*

The patient's disease was characterized by recurrent infections due to extracellular pyogenic bacteria. Standard immunological studies gave normal results, and major PMN defects (i.e., chronic granulomatous disease) were ruled out. Given that inherited IRAK-4 deficiency has been associated with recurrent infections (14–22), we analyzed the *IRAK4* gene in our patient.

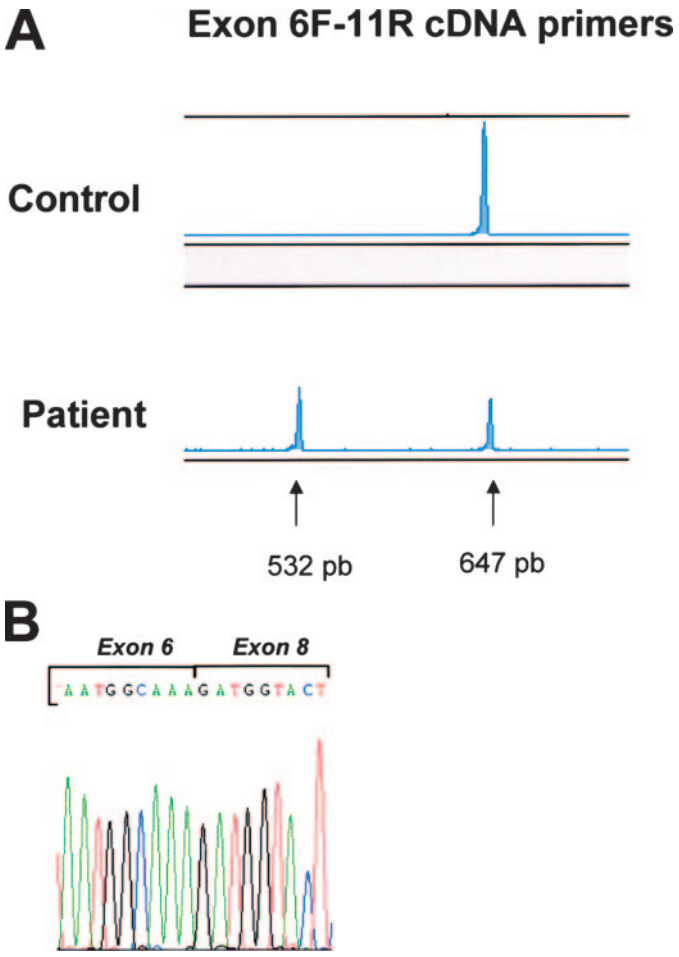

FIGURE 2. Mutation + 5 G>T in intron 7 induces exon (ex) 7 skipping. A, PCR amplification products using ex6F cDNA and ex11R cDNA primers and cDNA from a control and the patient were analyzed onto ABI310 DNA sequencer. A normal PCR product size (647 pb) and a truncated one (532 pb) were observed in our patient. *B,* Sequencing of the shortened band was performed using ex6F cDNA and ex11R cDNA nonfluorescent primers.

DNA sequencing revealed three mutations: one missense mutation resulting in the substitution of arginine by cysteine at position 12 (c. 34 C>T; p.Arg^{12}Cys); a second missense mutation at position 391 (c. 1170 G>A; p.Arg^{391}His); and an intronic mutation at position + 5 of intron 7 (G>T) (designated c.831 + 5 G>T) (Fig. 1, *A* and *B*). Analysis of DNA from the two parents showed that c. 34 C>T; p.Arg^{12}Cys was inherited from the father, along with p.Arg^{391}His, whereas c.831 + 5 G>T was inherited from the mother (Fig. 1*A*). Polyphen software (http://tux.embl-heidelberg.de/ramensky/polyphen.cgi) and SIFT software (http://blocks.fhcrc.org/sift/SIFT.html) both predicted a benign effect of the p.Arg^{391}His substitution and detrimental effect of the p.Arg^{12}Cys mutation. Indeed, the p.Arg^{12}Cys mutation involves a highly conserved residue that is located in the external region of the death domain of the protein

acid residue. *D,* Expression of IRAK-4 by Western blotting. A total of 2.5×10^6 cell equivalents were loaded in each well. After SDS-PAGE, the proteins were transferred to nitrocellulose membranes and incubated with anti-human IRAK-4 Ab at 1/500 dilution overnight. The Western blots were revealed as described in *Materials and Methods*.

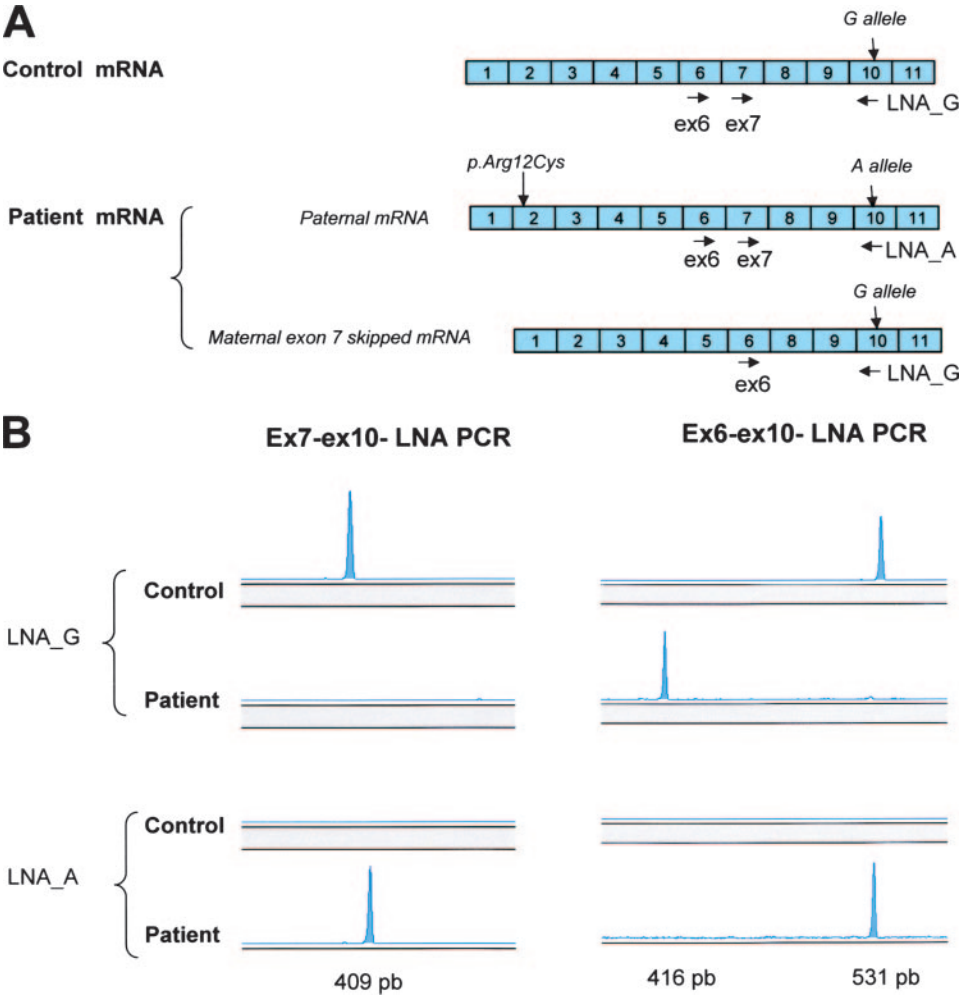

FIGURE 3. *A*, Full-length mRNA molecules are exclusively produced from the paternal allele. Allele-specific PCR was performed using two different reverse LNA primers. Ex10R LNA_G primer matches the wild-type allele (c.1170 G allele) whereas Ex10R LNA_A primer is specific of the variant allele (c.1170 A allele). The paternal mRNA contained the A allele and the maternal mRNA the G allele. The control used in this experiment was homozygous for the G allele. *B*, Fluorescent products obtained after PCR amplification of cDNA from the patient or the control were then analyzed on a ABI310 DNA sequencer. Expected PCR product sizes are indicated. The 416-bp peak observed with the Ex6F-Ex10R LNA_G set of primers corresponds to the exon 7-skipped form of mRNA.

(Fig. 1*C*). p.Arg^{391}His affects a nonconserved amino acid residue of the IRAK-4 kinase domain and is located near a previously described polymorphism (rs4251583, p.His^{390}Arg). In addition, the p.Arg^{391}His mutation does not alter mRNA splicing (data not shown). Although we cannot rule out the possibility that the presence of the two mutations on the same paternal allele has a detrimental effect on the protein function, our findings make it more likely that only p.Arg^{12}Cys is deleterious and that p.Arg^{391}His is a rare neutral variant.

RNA from the patient was further studied to assess the potential consequence of the c.831 + 5 G>T mutation. For this purpose, primers were designed in exons 6 and 11 and PCR products from the patient's cDNA were analyzed onto ABI310 (Fig. 2*A*). The presence of an abnormal band revealed that the intronic mutation resulted in a splice defect leading to the skipping of exon 7 and a predicted stop codon at position 249. Sequencing of the shortened PCR band confirmed the abnormal exon 6–8 junction (Fig. 2*B*). The observation of a relative abundance of a shortened mRNA without exon 7 as compared with full-length mRNA (see Fig. 2) argued against marked mRNA nonsense-mediated decay and could thus theoretically lead to the production of a truncated protein ending at position 248 (p.Cys^{240}MetfsX8).

The possibility that residual full-length RNA molecules were produced from the maternal allele was excluded by taking advantage of the patient's heterozygosity for the p.Arg^{391}His variant in exon 10. cDNA from the patient was amplified using LNA-modified primers with a C or a T at the 3′ end (thus specific for the wild-type allele G, ex10R LNA_G, or for the paternal allele A, ex10R LNA_A, Fig. 3*A*). Maternal mRNA molecules were theoretically specifically amplified using ex10R LNA_G and paternally derived mRNA, using ex10R LNA_A. The specificity of the LNA primers was confirmed using the ex7F and ex10 LNA primers as shown in Fig. 3*B*. PCR amplification was only observed with the ex7F and ex10 LNA_G primers in the control (homozygous for the wild-type allele, c.1170 G/G), whereas PCR amplification was positive in the patient using primers ex7F and ex10 LNA_A and negative using

Table I. *Absence of IRAK-4 function*[a]

	Mean Fluorescence Intensity	
	Controls	Patient
PBS	154.0 ± 4.7	159.1 ± 4.6
MALP-2 (TLR2/6)	237.2 ± 5.9[b]	162.0 ± 5.4
Pam3CSK4 (TLR1/2)	234.7 ± 3.8[b]	162.7 ± 4.9
LPS (TLR4)	264.1 ± 6.9[b]	165.0 ± 5.5
R-848 (TLR7/8)	285.3 ± 5.2[b]	165.7 ± 5.2
CpG-DNA (TLR9)	285.0 ± 6.2[b]	162.3 ± 6.5

[a] Whole-blood samples were incubated for 5 min at 37°C with PBS or with the following TLR agonists: LPS (10 ng/ml; TLR4); MALP-2 (10 ng/ml; TLR2/6); Pam3CSK4 (500 ng/ml; TLR1/2), R-848 (10 μg/ml; TLR7/8); or CpG-DNA (100 μg/ml; TLR9). Phospho-IRAK-1 content was then measured by flow cytometry on methanol-permeabilized cells as described in *Materials and Methods*. Results are expressed as mean ± SEM (n = 3; each experiment was performed with a different healthy control).

[b] Significantly different from samples incubated with PBS ($p < 0.05$).

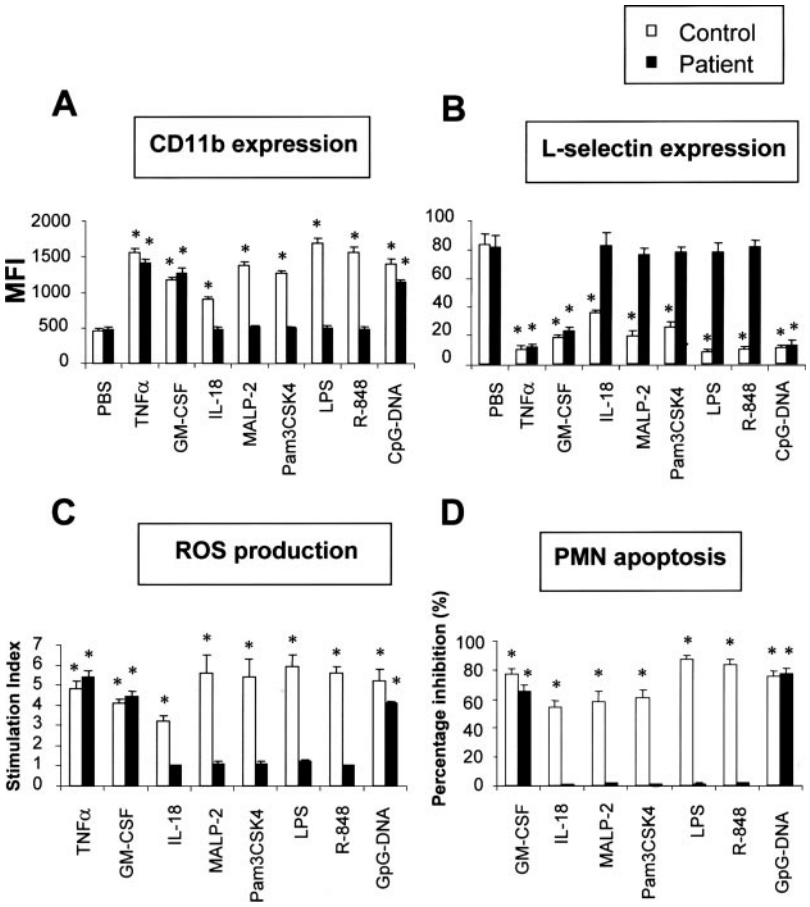

FIGURE 4. Impaired PMN functions in response to IL-18 and TLR agonists, except for TLR9. *A* and *B,* Adhesion molecule expression at the PMN surface: whole-blood samples were incubated at 37°C for 1 h with PBS, TNF-α (100 U/ml), GM-CSF (1000 pg/ml), IL-18 (500 ng/ml), or the following TLR agonists: LPS (10 ng/ml; TLR4), MALP-2 (10 ng/ml; TLR2/6), Pam3CSK4 (500 ng/ml; TLR1/2), R-848 (10 μg/ml; TLR7/8), or CpG-DNA (100 μg/ml; TLR9). Samples were then stained with PE-anti-CD11b and purified anti-L-selectin Abs at 4°C for 30 min. Results are expressed as MFI. ∗ Significantly different from sample incubated with PBS ($p < 0.05$). *C,* PMN oxidative burst: whole-blood samples were pretreated with HE for 15 min at 37°C and then incubated with TNF-α, GM-CSF, IL-18 or TLR agonists as described above, followed by fMLP stimulation (10^{-6} M, 5 min). Results are expressed as a stimulation index (ratio of the mean fluorescence intensity of stimulated cells to that of unstimulated cells). ∗, Significantly different from the sample incubated with PBS (stimulation index, 1; $p < 0.05$). *D,* PMN apoptosis. Whole-blood samples were incubated in 24-well tissue cultures plates at 37°C with 5% CO_2 for 8 h with PBS, GM-CSF, IL-18, or TLR agonists as described above. PMNs were identified by using an FITC-anti-CD15 Ab. Apoptosis was quantified by staining with allophycocyanin-annexin V and 7-AAD as described in *Materials and Methods*. Results are expressed as the percentage inhibition of PMN apoptosis [1 − (% of total annexin V^+ PMNs in stimulated sample/% of total annexin V^+ PMN in PBS-treated sample)] × 100. ∗, Significantly different from the sample incubated with PBS (percentage inhibition of apoptosis, 0; $p < 0.05$). All values represent three independent experiments, each with a different healthy control.

primers ex7F and ex10 LNA_G. These results confirmed that full-length mRNA molecules (containing exon 7) were exclusively produced from the paternal allele. They were confirmed by using Ex6F-ex10R LNA_G, that amplified only exon 7-truncated mRNA, and full-length mRNA molecules using Ex6F-ex10R LNA_A (Fig. 3*B*). Together, these data confirmed that full-length mRNA molecules were exclusively produced from the paternal allele and thus carried the (p.Arg^{12}Cys and p.Arg^{391}His) mutations.

Presence of a nonfunctional IRAK-4 protein

As expected, a band corresponding to an IRAK-4 protein of apparently normal molecular mass was detected by Western blotting of the patient's PMNs; no shortened protein was observed (Fig. 1*D*). As the first step of IRAK-4 activity is the phosphorylation of IRAK-1 (29), we studied the functionality of IRAK-4 protein by analyzing the phospho-IRAK-1 content of intact PMNs treated with TLR agonists in whole blood, by means of flow cytometry with a mouse anti-human phospho-IRAK-1 Ab. Incubation of whole blood from healthy controls with TLR agonists for 5 min significantly increased IRAK-1 phosphorylation as compared with PBS (Table I). In contrast, pretreatment of the patient's PMNs with all the TLR agonists, including the TLR9 agonist, did not modify IRAK-1 phosphorylation as compared with PBS. This result suggested that IRAK-4 was non functional.

Table II. *Impaired modulation of Mcl-1 and phospho-Bad expression in response to TLR agonists, except for TLR9*[a]

	Mean Fluorescence Intensity			
	Mcl-1		Phospho-Bad	
	Controls	Patient	Controls	Patient
PBS	74.3 ± 2.1	76.7 ± 2.7	57.7 ± 2.0	59.3 ± 4.1
MALP-2 (TLR2/6)	121.0 ± 3.8[b]	77.7 ± 3.2	90.3 ± 2.6[b]	59.7 ± 3.5
Pam3CSK4 (TLR1/2)	117.7 ± 2.0[b]	75.3 ± 3.8	89.0 ± 2.3[b]	60.0 ± 4.0
LPS (TLR4)	121.7 ± 5.2[b]	77.3 ± 2.8	90.7 ± 3.2[b]	62.7 ± 3.2
R-848 (TLR7/8)	124.3 ± 3.4[b]	77.7 ± 2.7	91.0 ± 5.5[b]	62.3 ± 5.2
CpG-DNA (TLR9)	123.7 ± 3.8[b]	106.7 ± 4.7[b]	90.3 ± 3.8[b]	80.3 ± 2.7[b]

[a] Whole-blood samples were preincubated at 37°C in a water bath with gentle agitation for 2 h (Mcl-1 expression) or 1 h (phospho-Bad expression) with PBS or with TLR agonists as described in the legend of Table I. Mcl-1 and phospho-Bad content was then measured by flow cytometry on methanol-permeabilized cells as described in *Materials and Methods.* Results are expressed as mean ± SEM ($n = 3$; each experiment was performed with a different healthy control). Values obtained with an irrelevant Ab of the same isotype or with nonimmune serum were subtracted.

[b] Significantly different from samples incubated with PBS ($p < 0.05$).

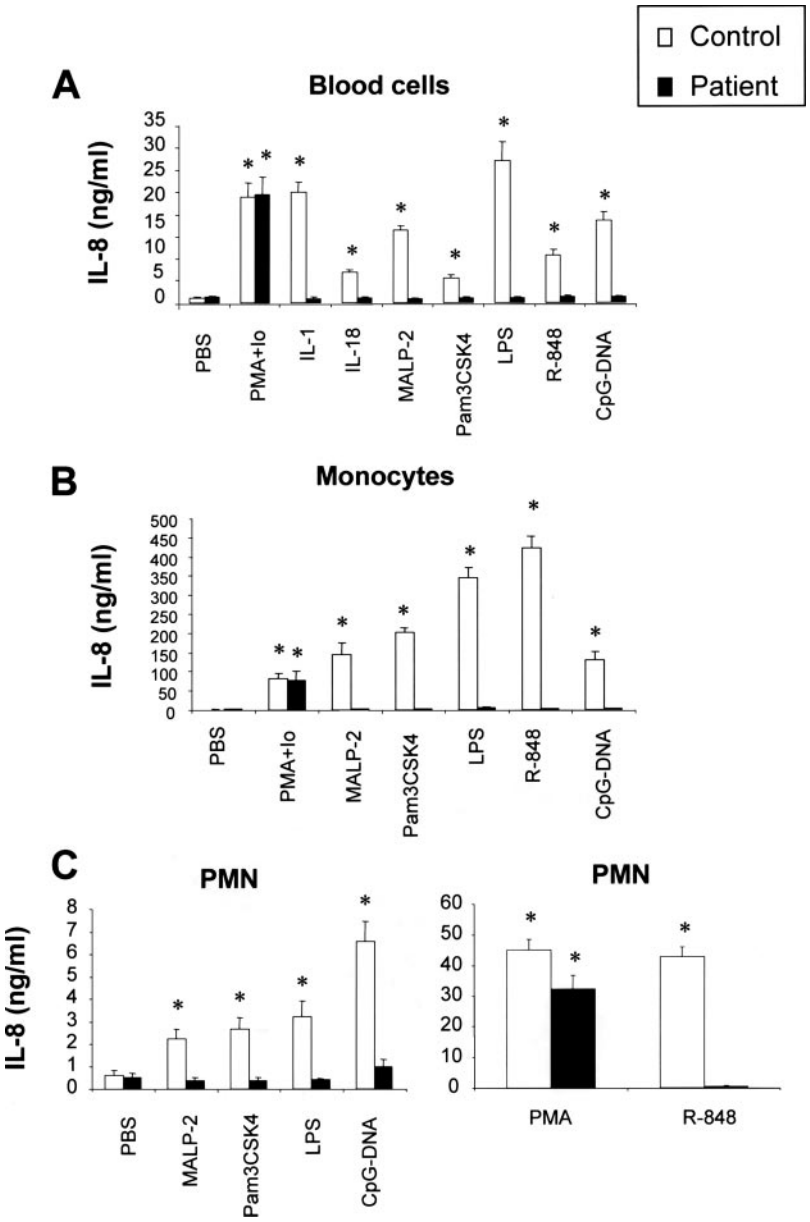

FIGURE 5. Impaired cytokine production by blood cells in response to TLR agonists, IL-1β and IL-18. Whole-blood samples (*A*), isolated monocytes (5×10^5/ml; *B*), and highly purified PMNs (5×10^6/ml; *C*) were incubated for 18 h with PMA-ionomycin (10^{-7}M and 10^{-5} M), PMA (10^{-7} M), IL-1β (50 ng/ml), IL-18 (500 ng/ml), or TLR agonists as described in the legend of Fig. 4. IL-8 production was measured by using the human inflammatory cytokine cytometric bead array (CBA) kit. *, Significantly different from the sample incubated with PBS ($p < 0.05$; $n = 3$, each experiment performed with a different healthy control).

Impaired PMN adhesion molecule expression and ROS production in response to IL-18 and TLR agonists, except for TLR9

PMN dysfunctions have been reported in IRAK-4 deficiencies (15), especially in response to LPS (TLR4), contrasting with normal responses to TNF. We therefore analyzed the effect of a broad range of TLR agonists on adhesion molecule expression and ROS production by PMNs. CD11b expression by resting patient's PMNs was normal, in keeping with normal chemotaxis and with the absence of leukocyte adhesion deficiency (not shown). In controls, incubation of whole-blood samples with TNF-α, GM-CSF, IL-18, and the TLR agonists, LPS (TLR4), MALP-2 (TLR2/6), Pam3CSK4 (TLR1/2), R-848 (TLR7/8) and CpG-DNA (TLR9), induced a significant increase in CD11b expression (Fig. 4*A*) and a significant decrease in L-selectin expression (Fig. 4*B*) related to activation-induced shedding of this molecule (30). In the patient, TNF-α and GM-CSF stimulation induced normal CD11b expression and normal L-selectin shedding at the PMN surface as compared with PBS-treated samples. In contrast, after treatment of patient's samples with IL-18 and the TLR agonists, LPS (TLR4), MALP-2 (TLR2/6), Pam3CSK4 (TLR1/2), and R-848 (TLR7/8), no significant increase in CD11b expression was observed as compared with the sample incubated with PBS. In addition, L-selectin was still detectable at the PMN surface, reflecting a defect in the shedding of this molecule. Surprisingly, however, the response to CpG-DNA (TLR9) was conserved (Fig. 4, *A* and *B*).

In controls, pretreatment of whole blood with TNF-α, GM-CSF, IL-18, or the various TLR agonists, followed by stimulation with fMLP, a structural analog of bacterial metabolic products, strongly increased ROS production (Fig. 4*C*). A similar increase in ROS production was also observed in the patient's PMNs after pretreatment with TNF-α or GM-CSF and stimulation with fMLP, ruling out defective priming of the phagocyte oxidative burst (31). This priming effect on the fMLP-stimulated PMN oxidative burst, which was also observed after treatment with CpG-DNA, was no longer detectable after incubation with the other TLR agonists or IL-18 (Fig. 4*C*).

Although the effect of TLR agonists on adhesion molecule expression and ROS production by monocytes is far lower than with

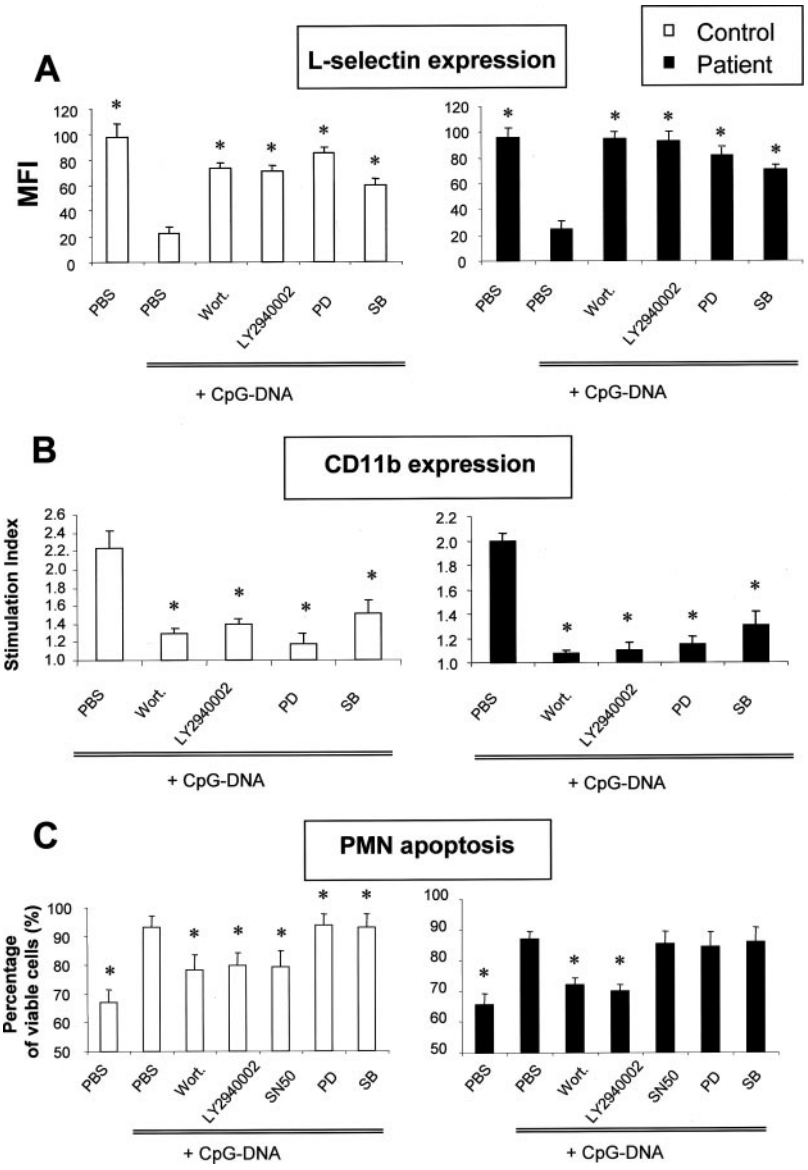

FIGURE 6. Involvement of the putative IRAK-4-independent PI3K signaling pathway in the persistent PMNs response to TLR9. *A* and *B,* Effect of kinase inhibitors on CpG-induced modulation of adhesion molecule expression at the PMN surface. Whole-blood samples were pretreated at 37°C with PBS, PI3K inhibitors (wortmannin (Wort.); 2500 nM; LY2940002; 25 μM), MEK1/2 inhibitor (PD98059; 50 μM) or p38MAPK inhibitor (SB203580; 25 μM) for 15 min and then with PBS or CpG-DNA for 1 h. L-selectin and CD11b expression at the PMN surface were then studied as described in the legend of Fig. 4. Results are expressed in MFI (L-selectin expression) and as a stimulation index (CD11b expression: ratio of the MFI of CpG-DNA-stimulated cells to that of unstimulated cells). *C,* Effect of an NF-κB inhibitor (SN50) and kinase inhibitors on CpG-DNA-induced PMN survival. Whole-blood samples were pretreated in 24-well tissue culture plates at 37°C in 5% CO_2-air with PBS, SN50 (100 μg/ml), PI3K inhibitors (wortmannin; 2500 nM; smf LY2940002; 25 μM), MEK1/2 inhibitor (PD98059: 50 μM) or p38MAPK inhibitor (SB203580; 25 μM) for 1 h. Samples were then incubated with PBS or CpG-DNA for 8 h. Survival was quantified as described in the legend of Fig. 4. Results are expressed as the percentage of viable cells (annexin V^--7-AAD^- cells). *, Significantly different from the CpG-DNA-stimulated sample incubated with PBS alone instead of kinase inhibitors ($p < 0.05$; $n = 3$, each experiment performed with a different healthy control).

PMNs, the patient's monocytes showed a pattern of responses similar to that of his PMNs, with altered responses to TLR agonists except for CpG-DNA (not shown).

Impaired prolongation of PMN survival by IL-18 and TLR agonists, except for TLR9

As PMN are usually very short-lived immune cells, prolongation of their lifespan by proinflammatory mediators is critical for their efficacy against pathogens (32). In keeping with previous reports (4, 33, 34), treatment of control PMNs for 8 h with GM-CSF, IL-18, and TLR agonists induced ~50–90% inhibition of PMN apoptosis in whole blood (total annexin V^+ cells); similar levels of inhibition were found in the early (annexin V^+-7-AAD^- cells) and late stage (annexin V^+-7-AAD^+ cells) of PMN apoptosis (not shown). In contrast, neither IL-18 nor LPS (TLR4), MALP-2 (TLR2/6), Pam3CSK4 (TLR1/2), and R-848 (TLR7/8) were able to inhibit the patient's PMN apoptosis (percentage inhibition of PMN apoptosis ~0%), whereas GM-CSF induced a normal prolongation of PMN survival. In keeping with the results for adhesion molecule expression and ROS production, the effect of CpG-DNA (TLR9) on the patient's PMN apoptosis was conserved (Fig. 4*D*).

We recently reported that the TLR-induced delay in PMN apoptosis was associated with modulation of Bcl-2 family members (4), with an increased level of the anti-apoptotic protein Mcl-1 and increased phosphorylation of the proapoptotic protein Bad, which have been reported to inhibit apoptosis (35). In our patient, although CpG-DNA (TLR9) induced a normal increase in Mcl-1 and phospho-Bad content, no modulation of either of these two proteins was observed after stimulation with the other TLR agonists, as compared with samples incubated with PBS (Table II).

Impaired cytokine production by PMNs and monocytes in response to IL-18, IL-1, and all TLR agonists

In keeping with previous data on patients with IRAK-4 deficiency (15, 16), we found strongly impaired proinflammatory cytokine (IL-8) production in the supernatant of the patient's whole-blood samples cultured with all TLR agonists, including CpG-DNA (Fig. 5*A*). Similar results were observed for IL-6, IL-1β, and TNF-α production (not shown).

As cytokine production by whole blood cells mainly reflects synthesis by monocytes, the patient's monocytes and PMNs were isolated and highly purified to analyze the individual response of the two cellular subpopulations to TLR agonists, and especially to

CpG-DNA (TLR9). As expected, IL-8 production by control monocytes incubated with TLR agonists was far higher than that of control PMN. Neither monocytes (Fig. 5*B*) nor PMNs (Fig. 5*C*) were able to produce significant amounts of IL-8 in response to LPS (TLR4), MALP-2 (TLR2/6), Pam3CSK4 (TLR1/2), or R-848 (TLR7/8). IL-8 production by the patient's PMNs and monocytes in response to CpG-DNA was also strongly diminished as compared with that of cells from a healthy control.

Finally, the parents' PMN exhibited normal responses (adhesion molecule expression, ROS production, delayed apoptosis, cytokine production) to all TLR agonists (not shown).

Involvement of direct stimulation of the PI3K pathway in the preserved PMN responses to TLR9

CpG-DNA induced normal responses by the patient's PMN in terms of survival, adhesion molecule expression, and ROS production, despite the lack of functional IRAK-4. This strongly suggested that an alternative pathway, independent of the classic TLR9/IRAK-4 pathway, was involved in TLR9 signaling. We therefore examined the effects of various kinase inhibitors on L-selectin and CD11b expression at the PMN surface, as well as on PMN apoptosis in whole blood incubated with CpG-DNA. These inhibitors were used at optimal concentrations previously determined in whole blood (4). Pretreatment with inhibitors of conventional protein kinase C (GF109203X: 5 μM), protein kinase Cδ kinase (rottlerin; 10 μM) and tyrosine kinase (genistein; 100 μM) had no effect on CpG-DNA-induced responses (not shown). In contrast, pretreatment of the patient's whole blood with PI3K inhibitors (wortmannin and LY2940002) suppressed the effect of CpG-DNA on PMN responses. CpG-DNA-induced shedding of L-selectin led to a significant decrease in L-selectin expression at the PMN surface as compared with PBS-treated samples (Fig. 6*A*); this decrease was totally abolished after preincubation of the patient's PMNs with PI3K inhibitors (the mean fluorescence intensity (MFI) of the sample incubated with PI3K inhibitors + CpG-DNA was similar to that observed after treatment with PBS alone; Fig. 6*A*). CpG-DNA-induced modulation of L-selectin expression was also significantly reduced after preincubation with PD98059 (an ERK1/2 kinase inhibitor) or SB203580 (a p38MAPK inhibitor). Similarly, the CpG-DNA-induced increase in CD11b expression (reflected by the increase in stimulation index; Fig. 6*B*) was significantly reduced after preincubation with PI3K inhibitors as well as with ERK1/2 kinase and p38MAPK inhibitors.

Finally, in keeping with previous data (4), the CpG-DNA-induced increase in the percentage of cell survival (annexin V^--7-AAD^- cells) was significantly reduced after preincubation of control samples with PI3K inhibitors and the NF-κB inhibitor SN50, whereas MAPK inhibitors did not affect PMN apoptosis (Fig. 6*C*). In the patient's PMNs, the inhibitory effect of PI3K inhibitors was conserved whereas the NF-κB inhibitor SN50, which strongly suppressed CpG-DNA-induced survival of control PMNs, had no effect on TLR9-induced survival of the patient's PMNs.

The PI3K inhibitor-induced reduction in PMN responses was also observed in healthy controls but at a lower level than in the patient (Fig. 6). This result suggested a critical role of the direct TLR9/PI3K pathway in the patient's PMN responses.

The effect of ERK1/2 kinase and p38MAPK inhibitors on CpG-DNA-induced modulation of adhesion molecule expression observed in control and the patient's PMNs strongly suggested the involvement of these kinases downstream of TLR9 activation. We therefore studied the phospho-ERKK1/2 and phospho-p38MAPK contents of intact PMN treated in whole blood, by means of flow cytometry. As shown in Fig. 7, incubation of whole blood from controls and the patient with CpG-DNA significantly increased

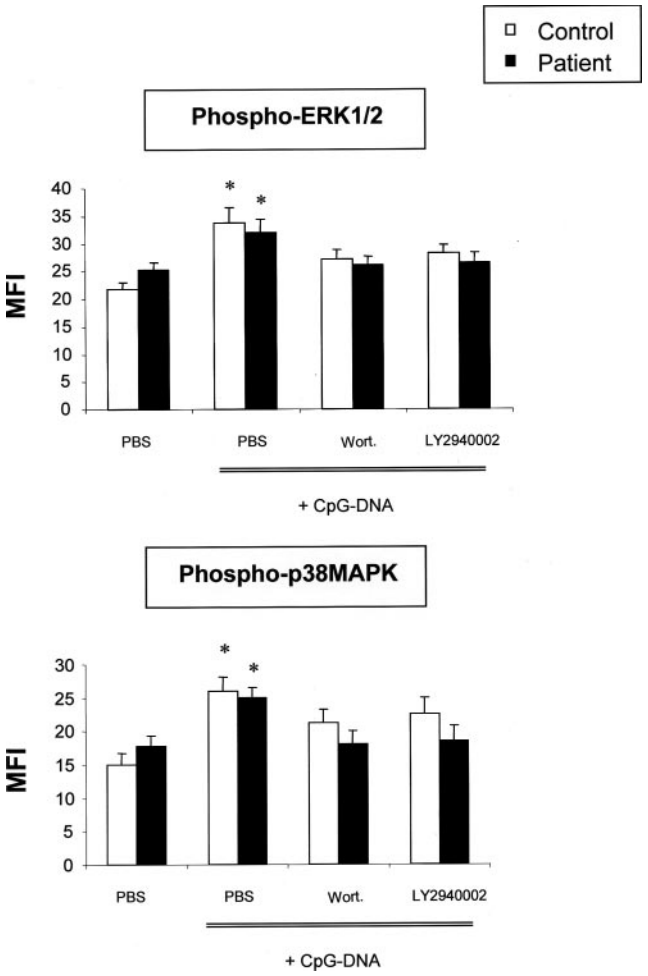

FIGURE 7. Effect of CpG-DNA on intracellular ERK1/2 and p38MAPK phosphorylation. Whole-blood samples were preincubated at 37°C in a water bath with PBS or PI3K inhibitors (wortmannin (wort); 2500 nM and LY2940002; 25 μM) for 15 min and then with PBS or CpG-DNA (100 μg/ml) for 10 min. Phospho-p38MAPK and phospho-ERK1/2 contents were then measured by flow cytometry on methanol-permeabilized cells as described in *Materials and Methods*. Results are expressed as the MFI. Values obtained with an irrelevant Ab of the same isotype were subtracted. Values are means ± SEM ($n = 3$, each experiment was performed with a different healthy control). *, Significantly different from samples incubated with PBS alone ($p < 0.05$).

ERK1/2 and p38MAPK phosphorylation after 10 min as compared with PBS. This effect was significantly reduced by preincubation with PI3K inhibitors. Total ERK1/2 and p38MAPK content, measured in the same conditions, was not modified by treatment with CpG-DNA (data not shown).

Discussion

We describe an inherited IRAK-4 deficiency in a patient with compound heterozygosity generating a nonfunctional IRAK-4 protein. PMN functional responses (adhesion molecule expression, ROS production, survival, and proinflammatory cytokine production) to MALP-2, Pam3CSK4, LPS, and R-848, which engage TLR2/6, TLR1/2, TLR4 and TLR7/8, respectively, were strongly impaired, as were PMN responses to IL-18 (the receptor of which shares the same intracytoplasmic TIR domain). In contrast, the patient's PMN responses to CpG-DNA (TLR9) were normal, except for cytokine production, suggesting the existence, in parallel to the MyD88/IRAK-4-dependent pathway, of a distinct TLR9-induced

transduction pathway regulating adhesion molecule expression, ROS production, and survival.

The patient's PMNs exhibited an impaired response to several agonists of the IL-1R family, and especially TLRs, whereas a normal response to other stimuli, including TNF, was observed. These results suggest that the patient has a defect in the common TIR signaling pathway, upstream of TRAF-6 and downstream of individual TIR membrane receptors. *IRAK4* gene analysis showed two compound heterozygous mutations in our patient. The maternally inherited mutation at position + 5 of intron 7 (G>T) was predicted to result in a protein of 248 aa, truncated of a large part of the kinase domain. However, no shortened band was observed on Western blots with a polyclonal Ab directed against the whole IRAK-4 protein. These results suggest that the truncated protein resulting from the maternal mutation is degraded as exon 7 skipped mRNA molecules were not subject to drastic nonsense-mediated decay. The two paternally inherited missense mutations, located in the death domain (p.Arg^{12}Cys) and in the kinase domain of IRAK-4 (p.Arg^{391}His), did not interfere with IRAK-4 synthesis: IRAK-4 protein was detected in the patient's PMNs by Western blot. However, none of the TLR agonists increased IRAK-1 phosphorylation, further demonstrating the nonfunction of IRAK-4 protein. These results suggest that the p.Arg12Cys missense mutation of the paternal allele may hamper protein-protein interactions via the death domain in the TIR pathway. Indeed, the p.Arg^{12}Cys mutation involves a residue that is located at the surface of the protein; this domain is thought to interact with the different ligands of IRAK-4 such as MyD88. This residue is highly conserved through evolution in IRAK-4 orthologous proteins including human, *Mus musculus, Bos taurus, Gallus gallus, Xenopus tropicalis, Danio rerio,* and *Euprymna scolopes* (supplementary data available on request) but is not conserved in paralogs of the IRAK family, suggesting that it participates to the specificity of interaction. It is therefore most likely that the substitution of this positively charged residue (arginine) by a neutral one (cysteine) interferes either with the conformation of the IRAK-4 death domain or with the interaction of IRAK-4 with its partners, preventing the assembly of an active signaling complex following TLR activation. pArg^{391}His, located in *cis* of the p.Arg^{12}Cys substitution, was predicted to be benign with two software programs based on structural and amino acid conservation and had no effect on mRNA splicing. A deleterious effect is thus unlikely, but a synergistic deleterious effect of the two missense mutations could not be excluded. The nonfunction of IRAK-4 protein in our patient was also confirmed by the absence of significant IKK phosphorylation, which results from TLR pathway activation (not shown).

TLR9-induced responses, i.e., adhesion molecule expression, ROS production and survival, were normal in the patient's PMN, whereas cytokine production was lower than with control PMN. This suggests that different pathways may be involved in these functions; in particular, the IRAK-4 dependent pathway is necessary for TLR9-induced cytokine production, whereas other functions might use independent pathways. PI3Ks have been reported to enhance nuclear translocation of NF-κB through phosphorylation and activation of IκB-kinase and activation of MAPK, especially in TLR2-stimulated PMN (13); nevertheless, it is not known whether MyD88/IRAK-4 complexes are required for this pathway. We clearly found that PI3K inhibitors (wortmannin and LY2940002) totally suppressed the effect of CpG-DNA on adhesion molecule expression and survival of our patient's PMN. These results suggest that TLR9 may be directly linked to PI3K, whereas the MyD88/IRAK-4-dependent pathway may be required for PI3K activation through the other TLRs. Such direct PI3K activation has been described for TLR2 in a human monocytic cell line (36).

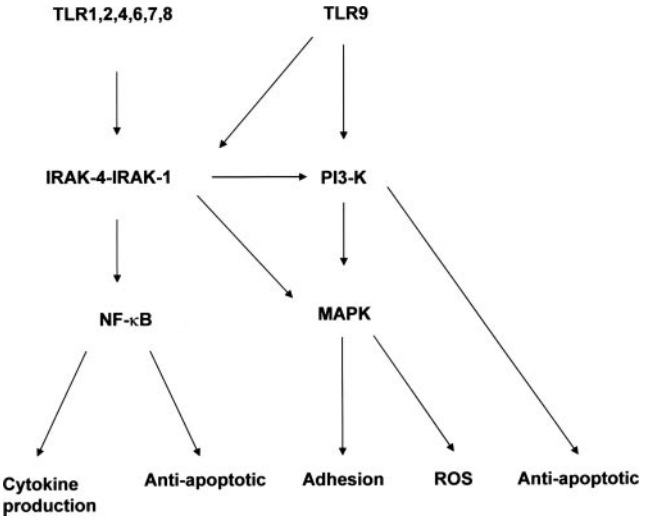

FIGURE 8. Scheme of CpG-DNA/TLR9-mediated cellular signaling in PMN. IRAK-4 dependent pathway. Recruitment of the TIR domain activates IRAK-4-TRAF6-TAK1 complex formation. This leads to the activation of both MAPKs and IKK complexes, culminating in up-regulation of transcription factors, including NF-κB. NF-κB activation leads to proinflammatory cytokine production and delays apoptosis. MAPK activation may be involved in the modulation of adhesion molecule expression at the PMN surface and in increased ROS production by primed PMNs. Wort, wortmannin. Alternative IRAK-4-independent pathway. Activation of class I PI3K (PI3K (I)-phosphatidylinositol 3,4,5-triphosphate/Akt/PKB) through TLR9 could be an alternative to the IRAK/IKK/NF-κB pathway. Its activation could lead to 1) delayed apoptosis through independent modulation of Bcl-2 family proteins and 2) recruitment of MAPKs involved in PMN adhesion and the oxidative burst.

The lipid products of PI3K, mainly phosphatidylinositol 3,4,5-triphosphate, induce translocation of Akt/PKB to the plasma membrane, where it is phosphorylated and activated by phosphatidylinositol 3,4,5-phosphate-dependent kinase (37). This pathway has been forwarded as a major mediator downstream of PI3K (38). In particular, Akt activation induces modulation of Bcl-2 family proteins such as Mcl-1 and phospho-Bad (39, 40) and could therefore be involved in the inhibitory effect of CpG-DNA on our patient's PMN apoptosis. In addition, it has been reported that class I PI3K-catalytic subunits can lead to phosphorylation of ERK1/2 and p38MAPK (9, 10, 41, 42); activation of these signaling pathways has been implicated in the up-regulation of CD11b expression (43, 44) and L-selectin shedding (45, 46) after PMN treatment with various inflammatory stimuli. In keeping with these data, we demonstrated that CpG-DNA-induced modulation of CD11b and L-selectin on the surface of our patient's PMNs is partially inhibited by pharmacological inhibitors of ERK1/2 and p38MAPK; furthermore, we found a CpG-DNA-induced increase in phosphorylation of ERK1/2 and p38MAPK in the patient's PMNs, which was reduced by PI3K inhibitors. These findings strongly suggest that IRAK-4-independent TLR9-induced PI3K activation leads to MAPK recruitment. Because CpG-DNA has no direct effect on ROS production, the use of kinase inhibitors did not allow us to analyze the involvement of MAPK in the priming effect of CpG-DNA on the PMN oxidative burst in response to fMLP. Nevertheless, PI3K products have also been reported to exert their effects on the PMN oxidative burst by activating downstream protein kinases such as Akt, which may directly phosphorylate components of the oxidase complex (47).

Taken together, our results suggest that activation of class I PI3K (PI3K (I)-phosphatidylinositol 3,4,5-phosphate-dependent

kinase/Akt/PKB) through TLR9, and subsequent recruitment of MAPK, could be an alternative pathway to the IRAK/IKK/NF-κB pathway involved in PMN adhesion, oxidative burst, and prolonged survival, which are major components of PMN functional activity. A schematic representation of the different pathways involved in PMN functions is proposed in Fig. 8. Nevertheless, we cannot formally exclude the involvement of other, unidentified signaling pathways leading to CpG-DNA-induced PMN responses. In particular, there is evidence of a TLR9-independent pathway leading to downstream PI3K activation and CD11b up-regulation in response to bacterial CpG-containing DNA in murine neutrophils (44, 48). This pathway described in human PMNs by Alvarez et al. (44) is MyD88 dependent and leads to IRAK-1 phosphorylation, suggesting the involvement of IRAK-4 in subsequent PI3K activation. However, we cannot formally exclude the possibility that the IRAK-4-independent activation of PI3K observed in our patient after CpG-DNA stimulation may be related to the existence of TLR9-independent mechanisms, thus implicating non-CpG molecular motifs in synthetic oligonucleotides.

IRAK-4-deficient patients suffer from pyogenic infections but are resistant to viruses, fungi, and parasites, as well as many other bacteria. It has been speculated that cell surface TLRs rapidly sense bacterial infections by recognizing bacterial cell wall constituents in the extracellular medium. In contrast, several lines of evidence suggest that molecular recognition of CpG-DNA occurs inside the cells (49). TLR9 might enter the phagosome from the endoplasmic reticulum (50) and bind bacterial DNA released into the phagosome following bactericidal processes. In addition, TLR9 was recently implicated in host defenses against intracellular pathogens (51, 52). Further studies are necessary to elucidate the role of direct PI3K activation by TLR9 in the phagosome, relative to cell surface activation of the TLRs-IRAK-4-dependent pathway in defenses against microorganisms, and especially intracellular pathogens. Nevertheless, we clearly observed that CpG-DNA induced normal PMN functions in terms of adhesion molecule expression and survival in our IRAK4-deficient patient, suggesting that the IRAK-4 dependent pathway may be compensated for by the TLR9-dependent IRAK-4-independent pathway. This may account, at least in part, for the observed clinical improvement with age.

In conclusion, this study provides the first description of persistent TLR9-induced responses, critically involved in antimicrobial defenses, by PMNs from a patient with inherited IRAK-4 deficiency. These results strongly suggest the existence of a TLR9 alternative pathway leading to PI3K activation independently of the classical MyD88-IRAK-4 pathway. This may explain the control of infections due to microorganisms other than pyogenic bacteria by PMNs in patients with inherited IRAK-4 deficiency. Finally, our study emphasizes the importance of lessons of nature in understanding the role of the TLR in human defenses.

Acknowledgments

We thank Steven and his family.

Disclosures

The authors have no financial conflict of interest.

References

1. Babior, B. M. 1984. Oxidants from phagocytes: agents of defense and destruction. *Blood* 64: 959–966.
2. Savill, J., I. Dransfield, C. Gregory, and C. Haslett. 2002. A blast from the past: clearance of apoptotic cells regulates immune responses. *Nat. Rev. Immunol.* 2: 965–975.
3. Hayashi, F., T. K. Means, and A. D. Luster. 2003. Toll-like receptors stimulate human neutrophil function. *Blood* 102: 2660–2669.
4. François, S., J. El Benna, P. M. C. Dang, M. A. Gougerot-Pocidalo, and C. Elbim. 2005. Inhibition of neutrophil apoptosis by Toll-like receptor agonists in whole blood: involvement of the phosphoinositide 3-kinase/Akt and NF-κB signaling pathways leading to increased levels of Mcl-1, A1 and phosphorylated Bad. *J. Immunol.* 174: 3633–3642.
5. Beutler, B. 2000. TLR4: central component of the sole mammalian LPS sensor. *Curr. Opin. Immunol.* 12: 20–26.
6. Akira, S. 2003. Toll-like receptor signaling. *J. Biol. Chem.* 278: 38105–38108.
7. Yum, H. K., J. Arcaroli, J. Kupfner, R. Shenkar, J. M. Penninger, T. Sasaki, K. Y. Yang, J. S. Park, and E. Abraham. 2001. Involvement of phosphoinositide 3-kinases in neutrophil activation and the development of acute lung injury. *J. Immunol.* 167: 6601–6608.
8. Zhu, D., H. Hattori, H. Jo, Y. Jia, K. K. Subramanian, F. Loison, J. You, Y. Le, M. Honczarenko, L. Silberstein, and H. R. Luo. 2006. Deactivation of phosphatidylinositol 3,4,5-triphosphate/Akt signaling mediates neutrophil spontaneous death. *Proc. Natl. Acad. Sci. USA* 103: 14836–14841.
9. Guha, M., and N. Mackman. 2002. The phosphatidylinositol 3-kinase-Akt pathway limits lipopolysaccharide activation of signaling pathways and expression of inflammatory mediators in human monocytic cells. *J. Biol. Chem.* 277: 32124–32132.
10. Fukao, T., and S. Koyasu. 2003. PI3K and negative regulation of TLR signaling. *Trends Immunol.* 24: 358–363.
11. Madrid, L. V., C. Y. Wang, D. C. Guttridge, A. J. Schottelius, A. S. Baldwin, and M. W. Mayo. 2000. Akt suppresses apoptosis by stimulating the transactivation potential of the RelA/p65 subunit of NF-κB. *Mol. Cell. Biol.* 20: 1626–1638.
12. Madrid, L. V., M. W. Mayo, J. Y. Reuther, and A. S. Baldwin. 2001. Akt stimulates the transactivation potential of the RelA/p65 subunit of NF-κB through utilization of the IκB kinase and activation of the mitogen-activated protein kinase p38. *J. Biol. Chem.* 276: 18934–18940.
13. Strassheim, D., K. Asehnoune, J. S. Park, J. Y. Kim, Q. He, D. Richter, K. Kuhn, S. Mitra, and E. Abraham. 2004. Phosphoinositide 3-kinase and Akt occupy central roles in inflammatory responses of Toll-like receptor 2-stimulated neutrophils. *J. Immunol.* 172: 5727–5733.
14. Medvedev, A. E., A. Lentschat, D. B. Kuhns, J. C. G. Blanco, C. Salkowski, S. Zhang, M. Arditi, J. I. Gallin, and S. N. Vogel. 2003. Distinct mutations in *IRAK-4* confer hyporesponsiveness to lipopolysaccharide and interleukin-1 in a patient with recurrent bacterial infections. *J. Exp. Med.* 198: 521–531.
15. Picard, C., A. Puel, M. Bonnet, C. L. Ku, J. Bustamante, K. Yang, C. Soudais, S. Dupuis, J. Feinberg, C. Fieschi, et al. 2003. Pyogenic bacterial infections in humans with IRAK-4 deficiency. *Science* 299: 2076–2079.
16. Currie, A. J., D. J. Davidson, G. S. D. Reid, S. Bharya, K. L. MacDonald, R. Devon, and D. P. Speert. 2004. Primary immunodeficiency to pneumococcal infection due to a defect in Toll-like receptor signaling. *J. Pediatr.* 144: 512–518.
17. Day, N., N. Tangsinmankong, H. Ochs, R. Rucker, C. Picard, J. L. Casanova, S. Haraguchi, and R. Good. 2004. Interleukin receptor-associated kinase (IRAK-4) deficiency associated with bacterial infections and failure to sustain antibody responses. *J. Pediatr.* 144: 524–526.
18. Enders, A., U. Pannicke, R. Berner, P. Henneke, K. Radlinger, K. Schwarz, and S. Ehl. 2004. Two siblings with lethal pneumococcal meningitis in a family with a mutation in interleukin-1 receptor-associated kinase 4. *J. Pediatr.* 145: 698–700.
19. Yang, K., A. Puel, S. Zhang, C. Eidenschenk, C. L. Ku, A. Casrouge, C. Picard, H. von Bernuth, B. Senechal, S. Plancoulaine, et al. 2005. Human TLR7-, -8-, and -9-mediated induction of IFN-α/β and -λ is IRAK-4 dependent and redundant for protective immunity to viruses. *Immunity* 235: 465–478.
20. Cardenes, M., H. von Bernuth, A. Garcia-Saavedra, E. Santiago, A. Puel, C. L. Ku, J. F. Emile, C. Picard, J. L. Casanova, E. Colino, et al. 2006. Autosomal recessive interleukin-1 receptor-associated kinase 4 deficiency in fourth-degree relatives. *J. Pediatr.* 148: 549–551.
21. Davidson, D. J., A. J. Currie, D. M. Bowdish, K. L. Brown, C. M. Rosenberger, R. C. Ma, J. Bylund, P. A. Campsall, A. Puel, C. Picard, et al. 2006. IRAK-4 mutation (Q293X): rapid detection and characterization of defective post-transcriptional TLR/IL-1R responses in human myeloid and non-myeloid cells. *J. Immunol.* 177: 8202–8211.
22. Ku, C. L., C. Picard, M. Erdos, A. Jeurissen, J. Bustamante, A. Puel, H. von Bernuth, O. Filipe-Santos, H. H. Chang, T. Lawrence, et al. 2007. *IRAK4* and *NEMO* mutations in otherwise healthy children with recurrent invasive pneumococcal disease. *J. Med. Genet.* 44: 16–23.
23. Amar, M., N. Amit, T. Pham Huu, S. Chollet-Martin, M. T. Labro, M. A. Gougerot-Pocidalo, and J. Hakim. 1990. Production by K562 cells of an inhibitor of adherence-related functions of human neutrophils. *J. Immunol.* 144: 4749–4756.
24. Rothe, G., and G. Valet. 1990. Flow cytometric analysis of respiratory burst activity in phagocytes with hydroethidine and 2′,7′-dichlorofluorescin. *J. Leukocyte Biol.* 47: 440–448.
25. Herault, O., P. Colombat, J. Domenech, M. Degenne, J. L. Bremond, L. Sensebe, M. C. Bernard, and C. Binet. 1999. A rapid single-laser flow cytometric method for discrimination of early apoptotic cells in a heterogenous cell population. *Br. J. Haematol.* 104: 530–537.
26. Elbim, C., H. Reglier, M. Fay, C. Delarche, V. Andrieu, J. El Benna, and M. A. Gougerot-Pocidalo. 2001. Intracellular pool of IL-10 receptors in specific granules of human neutrophils: differential mobilization by proinflammatory mediators. *J. Immunol.* 166: 5201–5207.
27. Grenier, A., M. Dehoux, A. Boutten, M. Arce-Vicioso, G. Durand, M. A. Gougerot-Pocidalo, and S. Chollet-Martin. 1999. Oncostatin M production and regulation by human polymorphonuclear neutrophils. *Blood* 93: 1413–1421.
28. Dang, P. M. C., C. Elbim, J. C. Marie, M. Chiandotto, M. A. Gougerot-Pocidalo, and J. El-Benna. 2006. Anti-inflammatory effect of interleukin-10 on human neutrophils involves inhibition of GM-CSF-induced $p47^{phox}$ phosphorylation through a decrease in ERK1/2 activity. *FASEB J.* 20: 1504–1516.

29. Suzuki, N., S. Suzuki, and W. C. Yeh. 2002. IRAK-4 as the central TIR signaling mediator in innate immunity. *Trends Immunol.* 23: 503–506.
30. Bevilacqua, M. P. 1993. Selectins. *J. Clin. Invest.* 91: 379–374.
31. Elbim, C., P. Rajagopalan-Levasseur, S. Chollet-Martin, J. L. Gaillard, M. Fay, J. Hakim, A. Fischer, J. L. Casanova, and M. A. Gougerot-Pocidalo. 1999. Defective priming of the phagocyte oxidative burst in a child with recurrent intracellular infections. *Microbes Infect.* 1: 581–587.
32. Haslett, C., J. S. Savill, M. K. Whyte, M. Stern, I. Dransfield, and L. C. Meagher. 1994. Granulocyte apoptosis and the control of inflammation. *Philos. Trans. R. Soc. London Biol. Sci.* 345: 327–333.
33. Derouet, M., L. Thomas, A. Cross, R. J. Moots, and S. W. Edwards. 2004. Granulocyte macrophage colony-stimulating factor signaling and proteasome inhibition delay neutrophil apoptosis by increasing the stability of Mcl-1. *J. Biol. Chem.* 279: 26915–26921.
34. Jablonska, E., M. Marcinczyk, and J. Jablonski. 2006. Toll-like receptors types 2 and 6 and the apoptotic process in human neutrophils. *Arch. Immunol. Ther. Exp.* 54: 137–142.
35. Perianayagam, M. C., V. S. Balakrishnan, B. J. Pereira, and B. L. Jaber. 2004. C5a delays apoptosis of human neutrophils via an extracellular signal-regulated kinase and Bad-mediated signaling pathways. *Eur. J. Clin. Invest.* 34: 50–56.
36. Arbibe, L., J. P. Mira, N. Teusch, L. Kline, M. Guha, N. Mackman, P. J. Godowski, R. J. Ulevitch, and U. G. Knaus. 2000. Toll-like receptor 2-mediated NF-κB activation requires a Rac1-dependent pathway. *Nat. Immunol.* 1: 533–540.
37. Cantley, L. C. 2002. The phosphoinositide 3-kinase pathway. *Science* 296: 1655–1657.
38. Toker, A., and L. C. Cantley. 1997. Signaling through the lipid products of phosphoinositide-3-OH kinase. *Nature* 387: 673–676.
39. del Peso, L., M. Gonzalez-Garcia, C. Page, R. Herrera, and G. Nunez. 1997. Interleukin-3-induced phosphorylation of BAD through the protein kinase Akt. *Science* 278: 687–689.
40. Schubert, K. M., and V. Duronio. 2001. Distinct roles for extracellular-signal-regulated protein kinase (ERK) mitogen-activated protein kinases and phosphatidylinositol 3-kinase in the regulation of Mcl-1 synthesis. *Biochem. J.* 356: 473–480.
41. Coxon, P. Y., M. J. Rane, D. W. Powell, J. B. Klein, and K. R. McLeisch. 2000. Differential mitogen-activated protein kinase stimulation by Fcγ receptor IIα and Fcγ receptor IIIβ determines the activation phenotype of human neutrophils. *J. Immunol.* 164: 6530–6537.
42. Rane, M. J., P. Y. Coxon, D. W. Powell, R. Webster, J. B. Klein, W. Pierce, P. Ping, and K. R. McLeisch. 2001. p38 kinase-dependent MAPKAPK-2 activation functions as 3-phosphoinositide-dependent kinase-2 for Akt in human neutrophils. *J. Biol. Chem.* 276: 3517–3523.
43. Mocsai, A., Z. Jakus, T. Vantus, G. Berton, C. A. Lowell, and E. Ligeti. 2000. Kinase pathways in chemoattractant-induced degranulation of neutrophils: the role of p38 mitogen-activated protein kinase activated by Src family kinase. *J. Immunol.* 164: 4321–4331.
44. Alvarez, M. E., J. I. Bass, J. R. Geffner, P. X. Calotti, M. Costas, O. A. Coso, R. Gamberale, M. E. Vermeulen, G. Salamone, D. Martinez, et al. 2006. Neutrophil signaling pathways activated by bacterial DNA stimulation. *J. Immunol.* 177: 4037–4046.
45. Fan, H., and R. Derynck. 1999. Ectodomain shedding of TGF-α and other transmembrane proteins is induced by receptor tyrosine kinase activation and MAP kinase signaling cascades. *EMBO J.* 18: 6962–6972.
46. Smolen, J. E., T. K. Petersen, C. Koch, S. J. O'Keefe, W. A. Hanlon, S. Seo, D. Pearson, M. C. Fossett, and S. I. Simon. 2000. L-selectin signaling of neutrophil adhesion and degranulation involves p38 mitogen-activated protein kinase. *J. Biol. Chem.* 26: 15876–15884.
47. Chen, Q., D. W. Powell, M. J. Rane, S. Singh, W. Butt, J. B. Klein, and K. R. McLeish. 2003. Akt phosphorylates $p47^{phox}$ and mediates respiratory burst activity in human neutrophils. *J. Immunol.* 170: 5302–5308.
48. Trevani, A. S., A. Chorny, G. Salamone, M. Vermeulen, R. Gamberale, J. Schettini, S. Raiden, and J. Geffner. 2003. Bacterial DNA activates human neutrophils by a CpG-independent pathway. *Eur. J. Immunol.* 33: 3164–3174.
49. Wagner, H. 2004. The immunobiology of the TLR9 subfamily. *Trends Immunol.* 25: 381–386.
50. Leifer, C. A., M. N. Kennedy, A. Mazzoni, C. W. Lee, M. J. Kruhlak, and D. M. Segal. 2004. TLR9 is localized in the endoplasmic reticulum prior to stimulation. *J. Immunol.* 173: 1179–1183.
51. Khan, I. A. 2007. Toll road for *Toxoplasma gondii*: the mystery continues. *Trends Parasitol.* 23: 1–3.
52. von Meyenn, F., M. Schaefer, H. Weighardt, S. Bauer, C. J. Kirschning, H. Wagner, and T. Sparwasser. 2006. Toll-like receptor 9 contributes to recognition of *Mycobacterium bovis* Bacillus Calmette-Guérin by Flt3-ligand generated dendritic cells. *Immunobiology* 211: 557–565.